South African Journal of Botany 186 (2025) 422–435

Contents lists available at ScienceDirect

South African Journal of Botany

journal homepage: www.elsevier.com/locate/sajb

Phytochemical profiling of saline cultivated *Tetragonia decumbens* Mill: In vitro cytotoxicity, acetylcholinesterase inhibitory activity, anti-cancer and anti-inflammatory potential

Avela Sogoni [a,*], Muhali Olaide Jimoh [a], Nasifu Kerebba [b], Sihle Ngxabi [a], John Paul Giesy [c,d,e], Rialet Pieters [f], Suranie Horn [g], Learnmore Kambizi [a], Charles Petrus Laubscher [a]

[a] Department of Horticultural Sciences, Cape Peninsula University of Technology, Symphony Way (off Robert Sobukwe Road), Bellville, 7535, South Africa
[b] Department of Chemistry, Makerere University, Kampala 7062, Uganda
[c] Department of Environmental Science, Baylor University, Waco, TX, USA
[d] Department of Veterinary Biomedical Sciences and Toxicology Centre, University of Saskatchewan, Saskatoon, Saskatchewan S7N 5B3, Canada
[e] Department of Integrative Biology and Center for Integrative Toxicology, Michigan State University, 1129 Farm Lane Road, East Lansing, MI, USA
[f] Unit for Environmental Sciences and Management, Faculty of Natural and Agricultural Sciences, North-West University, Private Bag X6001, Potchefstroom, North West 2520, South Africa
[g] Occupational Hygiene and Health Research Initiative, Faculty of Health Science, North-West University, Private Bag X6001, Potchefstroom, North West 2520, South Africa

ARTICLE INFO

Edited by: Prof U. Çakılcıoğlu

Keywords:
Aizoaceae
Alzheimer's disease
Cancer
Cytotoxicity
Edible halophyte
Functional food
Chronic inflammation

ABSTRACT

Cancer, Alzheimer's disease and chronic inflammation present considerable health issues for individuals worldwide. Current treatment with synthetic drugs has been associated with adverse side effects. Thus, the search for plant-based options that are affordable, reliable, and safe is highly imperative. This study explored the phytochemical profiling of ethanolic extracts of *Tetragonia decumbens*, their cytotoxicity, as well as their acetylcholinesterase inhibitory activity, anti-cancer and anti-inflammatory potential. Phenolic compounds in leaf extracts collected from samples cultivated in saline (0, 50, 100, 150, 200 and 250 mM NaCl) were identified with ultra-performance liquid chromatography-mass spectrometry (UPLC-MS). Cytotoxicity of the extracts against cancerous and non-cancerous cell lines was evaluated with the MTT (3-(4,5-dimethylthiazol-2-yl)-2,5-diphenyl tetrazolium bromide) cell viability assay. Lastly, the anti-inflammatory potency of the extracts against lipopolysaccharide induced macrophage cell line (RAW 264.7) was determined by monitoring the reduction of nitrites, while acetylcholinesterase inhibitory activity of the extract on H4IIE-*luc* cells was evaluated with the Ellman colorimetric method. For the first time, the UPLC-MS analysis identified 98 compounds in *T. decumbens,* most of which were flavonoids, flavonols, amino acids, hydroxybenzoic acid derivatives, and organic and fatty acids. A potent anti-inflammatory activity (27 μM) was observed at a dose of 100 μg/mL in the crude extract of plants grown in 100 mM NaCl, which was substantially higher than that of cells treated with aminoguanidine (35 μM) a positive control. There was also a significant inhibitory activity on acetylcholinesterase in cells treated with crude extracts of 0 mM NaCl (0.00031 mg/protein), followed by 50 mM NaCl (0.0016 mg/protein) and 100 mM NaCl (0.0031 mg/protein), respectively, compared with untreated cells (0.022 mg/protein). Additionally, the extract of 150 mM NaCl treatment showed a cytotoxic effect against cancer (34.3 %) and non-cancer (9.2 %) cells at a concentration of 1 mg/mL, and was not remmended for use due to toxicity concern on non-cancer cells. These findings suggest that the identified compounds in *T. decumbens* extracts could have potential anti-inflammatory and acetylcholinesterase inhibitory activities. Consequently, these compounds can be further explored as promising therapeutic agents for the dual treatment of inflammation and Alzheimer's disease.

* Corresponding author:.
E-mail address: sogonia@cput.ac.za (A. Sogoni).

https://doi.org/10.1016/j.sajb.2025.09.010
Received 28 June 2025; Received in revised form 10 August 2025; Accepted 8 September 2025
Available online 23 September 2025

1. Introduction

Inflammation is fundamentally a protective reaction to infections and tissue damage (Borquaye et al., 2020). During the initial stages of this process, macrophages serve as the primary line of defence, generating numerous pro-inflammatory mediators, including cytokines, nitric oxide, and prostaglandins, in response to stimuli such as microbial lipopolysaccharides (LPS) (Silva et al., 2021). In normal circumstances, the release of these molecules is critically important, occurring acutely and transiently in response to cell damage until the detrimental stimuli are resolved (Jo and Choi, 2024). However, the aberrant synthesis of these pro-inflammatory mediators over an extended duration can lead to chronic inflammation-related disorders (Achasih Quinta Nkemzi et al., 2024). Non-steroidal anti-inflammatory drugs potentially prevent the production of these pro-inflammatory mediators (Gonfa et al., 2023), but extended use in treating chronic inflammation has adverse consequences. This has led to a demand for novel treatments with minimal side effects. Natural compounds from medicinal plant species have been reported to effectively treat inflammatory-related illnesses with minimal side effects (Kim et al., 2024).

The degeneration of neurological function caused by the reduction of acetylcholine in the brains of the elderly results in a loss of cognitive ability (Chauhan et al., 2024; Nguyen et al., 2020). This condition is referred to as Alzheimer's disease (AD) and is the most common form of dementia (Rani et al., 2025). Primary intervention in treating AD focuses on regulating acetylcholine within the synaptic region to restore deficient cholinergic neurotransmission (Huang et al., 2022). Synthetic medicines such as tacrine, donepezil, and rivastigmine, used to regulate acetylcholine, are known to cause gastrointestinal disturbances. However, plant-based extracts with strong acetylcholinesterase (AChE) inhibitory activity have been reported to enhance acetylcholine levels in synaptic regions of the body (Prasathkumar et al., 2022). As a result, the pursuit of novel AChE inhibitors, especially those from natural sources, with enhanced potency persists.

In addition to chronic inflammation and Alzheimer's disease, cancer remains one of the leading causes of death worldwide, with mortality rising, especially in developing countries (Soerjomataram et al., 2023), thereby underscoring the urgent need for effective anticancer therapies. Chemotherapy and advancements in anticancer pharmaceuticals have enhanced patient care (Anand et al., 2023), but these have undesirable side effects in patients, such as vomiting, nausea, and alopecia (Guchhait et al., 2022). Recently, medicines of natural origin have been recommended as anti-cancer adjuvant therapies due to their anti-proliferative and pro-apoptotic properties (Chimento et al., 2023). These include plant compounds such as podophyllotoxin, vincristine, etoposide, irinotecan, vinblastine, topotecan, and paclitaxel, which have significantly contributed to the development of efficient anticancer pharmaceuticals (M.O. Jimoh et al., 2024). Bioactive compounds of plant origin, such as gimatecan and topotecan, are currently undergoing clinical research for cancer treatment due to their targeted efficacy (Asma et al., 2022). Nonetheless, not all plant species with anticancer potential have been fully investigated.

Edible halophytes recently gained popularity as a food source with functional capabilities due to their nutritional constituents and medicinal compounds (Ngxabi et al., 2025). These species are effective in treating chronic conditions such as cognitive impairment, metabolic disorders, cardiovascular complications, cancer and diabetes (Custodio et al., 2022). A neglected edible halophyte, *Tetragonia decumbens* Mill. commonly known as Dune spinach (English) and Duinespinasie (Afrikaans) in South Africa has been cultivated under saline conditions. The plant belongs to Aizoaceae, the largest succulent plant family, most of which are endemic to South Africa, tropics and sub-tropics (El-Raouf, 2021; Powell et al., 2018). This species demonstrated encouraging production returns and enhanced nutritional quality, showing promise for bio-saline agriculture (Sogoni et al., 2024). Nonetheless, a comprehensive profiling of its phytochemicals and their biological activities remains unexplored. Thus, the goal of this study was to elucidate the chemical profile of metabolites aggregated in the crude extracts of *T. decumbens* as well as their cytotoxicity, acetylcholinesterase inhibitory activity, anti-cancer and anti-inflammatory potential to further support its propagation, consumption, and commercialisation.

2. Materials and methods

2.1. Cultivation of T. decumbens

2.1.1. Plant material preparation, growth conditions and treatments

Tetragonia decumbens was identified by Prof. Charles Laubscher and allocated a voucher number 6162 at the Cape Peninsula University of Technology Herbarium, Bellville, South Africa. The plants used for this study were produced from cuttings using the method outlined by A. . Thereafter, the plants were subjected to saline conditions (0, 50, 100, 150, 200 and 250 mM NaCl) recently reported by Sogoni et al. (2024). After four months of saline treatment, plant leaves were harvested, desiccated, and pulverised for subsequent analysis.

2.2. Plant extraction

Approximately 10 g of pulverised *T. decumbens* leaves from each salt treatment were added to a spherical flask containing 200 mL of 70 % ethanol and shaken violently with an orbital shaker at 120 rpm for 48 h. The mixture was subsequently filtered and concentrated following the method of K. . The concentrated samples were preserved at 4 °C in the refrigerator and used in all analyses.

2.3. Phytochemical analysis using ultra-performance liquid chromatography-mass spectrometry (UPLC-MS)

The LC-MS analysis utilised a QA Waters Synapt G2 quadrupole time-of-flight mass spectrometer (MS). It was equipped with a Waters ultra-pressure liquid chromatography (UPLC) system utilising Waters MS^E technology and photodiode array detection. The phenolic compounds were identified using the method and instrument parameters adopted from M.O. employing negative ion mode with modest alterations. In the positive ion mode, both mobile phases consisted of 0.1 % formic acid, with water as mobile phase A and acetonitrile as mobile phase B. After 0.5 min of 100 % solvent A, the gradient shifted to 100 % B from 0.5 in to 12.5 min. After 13 min into the runtime, it changed to 100 % A for the next 2 min. The total run duration was 15 min. The flow rate was 0.4 mL/min; the seal wash was 5 min, and the column temperature was maintained at 55 °C. Electrospray ionisation was used in positive and negative ion modes with a desolvation temperature of 275 °C, desolvation gas at 650 L/h and the cone voltage of 15 V. Leucine encephalin was injected as a lock mass in the background and sodium formate was used for calibration to achieve accurate mass measurements. The MassLynx version 4.1 software platform supplied with Waters mass spectrometers was used to process each chromatogram manually.

2.3.1. Identification of phenolic compounds with UPLC-MS

The identified metabolites were assigned preliminary names based on matches with accurate masses of known compounds that match data in databases such as NIST, massBank, Metlin, and other repositories like PubChem, as well as mass fragmentation patterns of compounds and the number of carbon atoms for isotope relative abundance. Knowledge of the accurate mass allows prediction of unique formulas, but does not allow prediction of structures so it is not possible to accurately identify compounds based on the formula alone. In fact a single formula might have as many as 50 or more possible compounds. To identify compounds and assign UPAC names requires deconvolution of the mass fragment pattern in the MS-2 data. Tentative identification of compounds was made based on accurate mass matching, provided their accurate mass error (AME) exceeded 5 ppm. Then, the list of possible compounds was

reduced based on retention time, mass fragmentation, and ionisation modes. Also, several standards of phenolic compounds were introduced under uniform LC/MS settings for both positive and negative ion modes. Given the capability to obtain all standards and detect numerous compounds by UPLC-MS, the MS and MS^2 fragment ions of analogous compounds were utilised for annotation. Compound structures were clarified using MS-MS analysis of the sample's compounds, which were fragmented to correspond with product ion mass spectra. After obtaining isotope abundances, the quantity of carbon atoms in the peak was calculated as a confirmation step (Kerebba et al., 2022).

2.4. Cytotoxicity

2.4.1. MTT (3-[4.5-dimethylthiazol-2-yl]−25 diphenyl tetrazolium bromide) cell viability assay

The cancer cell line used is the genetically modified rat hepatoma cell line, H4IIE-*luc* (Aarts et al., 1993). It is assumed that the nature of its genetic modification would not interfere with the cell's viability since it is focused on expressing a firefly gene in the presence of aryl-hydrocarbon receptor (AhR) ligands. The AhR is endogenous to this cell line. The Vero cell line is non-cancerous and derived from African green monkey kidney cells. The cell line was obtained from the American Type Culture Collection (ATCC) (Manassas, VA, USA) (HB-8065). The cells were cultured with Dulbecco's Modified Eagle's Medium (DMEM) (Sigma, Darmstadt) supplemented with 10 % foetal bovine serum (FBS) (Thermo Scientific, USA) in a humidified incubator with 5 % CO_2 at 37 °C (Prinsloo et al., 2013). All experimental work was done aseptically. Cells were seeded at a density of 80,000 cells/mL into a transparent 96-well microplate and after 24 h, the cells were exposed to six extract concentrations (0.03125, 0.0625, 0.125, 0.25, 0.5 and 1 mg/mL plant equivalent) from each salt treatment (0, 50, 100, 150, 200 and 250 mM NaCl) in triplicate and incubated for 24 h. Each plate also had a set of wells representing the positive control, which were cells receiving only nutrient medium and a negative control cells that received nutrient medium only, but were killed purposely at the end of the experiment to have the absorbance of wells with dead cells.

After exposure, the medium was replaced with 0.5 mg/mL MTT and incubated for 30 min. Live cells metabolise the yellow tetrazolium bromide to a purple, formazan product using NAD(P)H-dependent cellular oxidoreductase enzymes. The insoluble formazan product was solubilised with dimethyl sulphoxide (DMSO) and the absorbance of each well quantified at 560 nm using a Berthold multi-mode microplate reader (TriStar LB941). Viability was expressed as a percentage of the exposed test media to the positive control absorption, after the absorption of the negative control wells was subtracted from all wells.

2.5. Anti-inflammatory activity

With a few minor adjustments, the approach of Nethengwe et al. (2024) was used to assess the anti-inflammatory potency of extracts. In 96-well plates, RAW 264.7 (ATCC TIB-71) cells (mouse tumour) were cultured in RPMI 1640 media enriched with 10 % foetal bovine serum. The cells were then allowed to adhere overnight. The next day, the utilised growth material was disposed of, and 50 μL of sample aliquots were added to the wells in quadruplicates, diluted in RPMI complete medium, to reach final concentrations of 50, 100, and 200 μg/mL. Thereafter, 50 μL of medium containing lipopolysaccharide (500 μg/mL) was added to the indicated wells to assess the anti-inflammatory efficacy. Cells were cultured for 24 h with the positive control, aminoguanidine (AG), at a concentration of 100 μM. To quantify the generation of nitric oxide (NO), 50 μL of the wasted culture media was moved to a fresh 96-well plate. N-(1-naphtyl)-ethylenediamine dihydrochloride (NED) solution and sulfanilamide solution were prepared in accordance with the manufacturer's instructions. The wasted culture medium was mixed with 50 μL of sulfanilamide solution and incubated for 10 min. Thereafter, each well received 50 μL NED solution and was incubated for a further ten minutes in the dark. A BioTek® PowerWave XS spectrophotometer was used to measure absorbance at 540 nm. The amount of NO in each sample was determined using a nitrite standard curve that was created from sodium nitrite diluted in a culture medium. The MTT assay was also used to measure the toxicity of the extract concentrations against RAW 264.7 cells to confirm that toxicity was not a contributing factor.

2.6. Acetylcholinesterase (AChE) activity

With a few adjustments, the spectrophotometric approach described by G.L. was used to measure the AChE activity. H4IIEluc cells were seeded in 12-well clear bottom cell culture microplates at 80,000 cells/mL, and after 24 h, the cells were exposed to 0.03 mg/mL plant equivalents in triplicate, trypsinised and harvested from the plate. The cells were centrifuged at 1000 g and the supernatant discarded. The cell pellets were resuspended in ice-cold potassium phosphate buffer (0.09 M K_2HPO_4 & 0.09 M KH_2PO_4) at pH 7.4. The resuspended cells were sonicated for 30 s to lyse them. The mixture was centrifuged at 4 °C at 10,000 g, and the supernatant was harvested for AChE activity and protein content determination. Both the AChE determination and protein content determination were done in the dark.

AChE determination was adapted for 96-wells where white-walled, clear flat-bottom microplates were used. Each well received 210 μL potassium phosphate buffer, 10 μL 30 mM acetylthiocholine iodide and 10 μL 10 mM Ellman's reagent and was incubated for 5 min at 37 °C before 10 μL sample supernatant was added. Each well harvested from the 12-well plate (in which exposure took place) was dosed in triplicate. This was done as fast as possible because the enzyme activity starts immediately. Absorbance was measured at 412 nm every minute for 6 min starting at time zero (7 points in total) using a SpectrMax®iD3 multimode microplate reader. To calculate AChE activity, the mean absorbance of each time interval was determined for the samples, lysate from untreated cells (cells received only nutrient media) and experimental blanks (wells with potassium phosphate buffer, acetylthiocholine iodide and Ellman's reagent but without cell lysate). This was followed by calculating the reaction gradient to determine the reaction rate. These values were normalised against protein content in each cell lysate and expressed as AChE activity in absorbance/min/mg protein.

The protein content of each of the exposure wells was determined using the Bradford Assay Kit. A protein standard calibration series was prepared using bovine serum albumin (BSA), serially diluted 1:1 to create a concentration series of 0–2000 μg/mL. 5 μL of the protein standard, and cell lysate were added to white walled 96-well microplates to which 245 μL Bradford's reagent was added. Absorbance was quantified at 590 nm using the Berthold multimode microplate reader (TriStar LB941). The absorbance of the protein standard was plotted on the y-axis against the protein standard concentration on the x-axis. The sample protein content was determined using the straight-line formula of the standard curve.

2.7. Statistical analysis

All data were statistically analysed with Minitab 18 statistical software. A one-way analysis of variance was used to assess the significance of treatment differences. Before applying parametric statistics, assumptions were validated by use of the Kolmogorov-Smirnov test to check for normality, while Levine's test was used to confirm homogeneity of variance. Using Tukey's (LSD) test, all significance assertions were evaluated with a type I error with probability of $p < 0.05$.

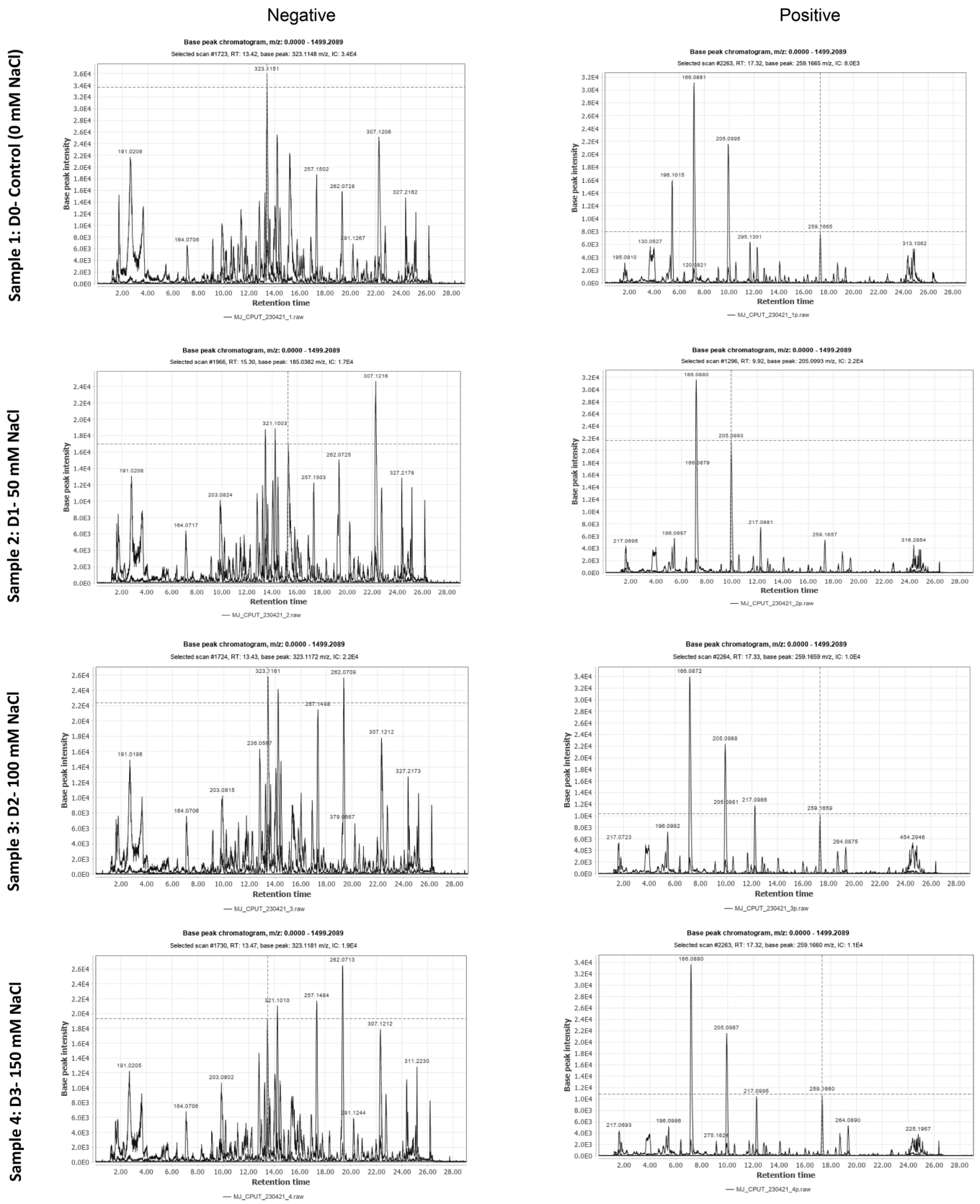

Fig. 1. UHPLC-ESI-MS base peak chromatograms of ethanol extracts of T. decumbens grown under saline conditions (0–250 mM NaCl) analysed in positive and negative ion modes. Cytotoxicity of *T. decumbens* crude extracts against cancerous and non-cancerous cells.

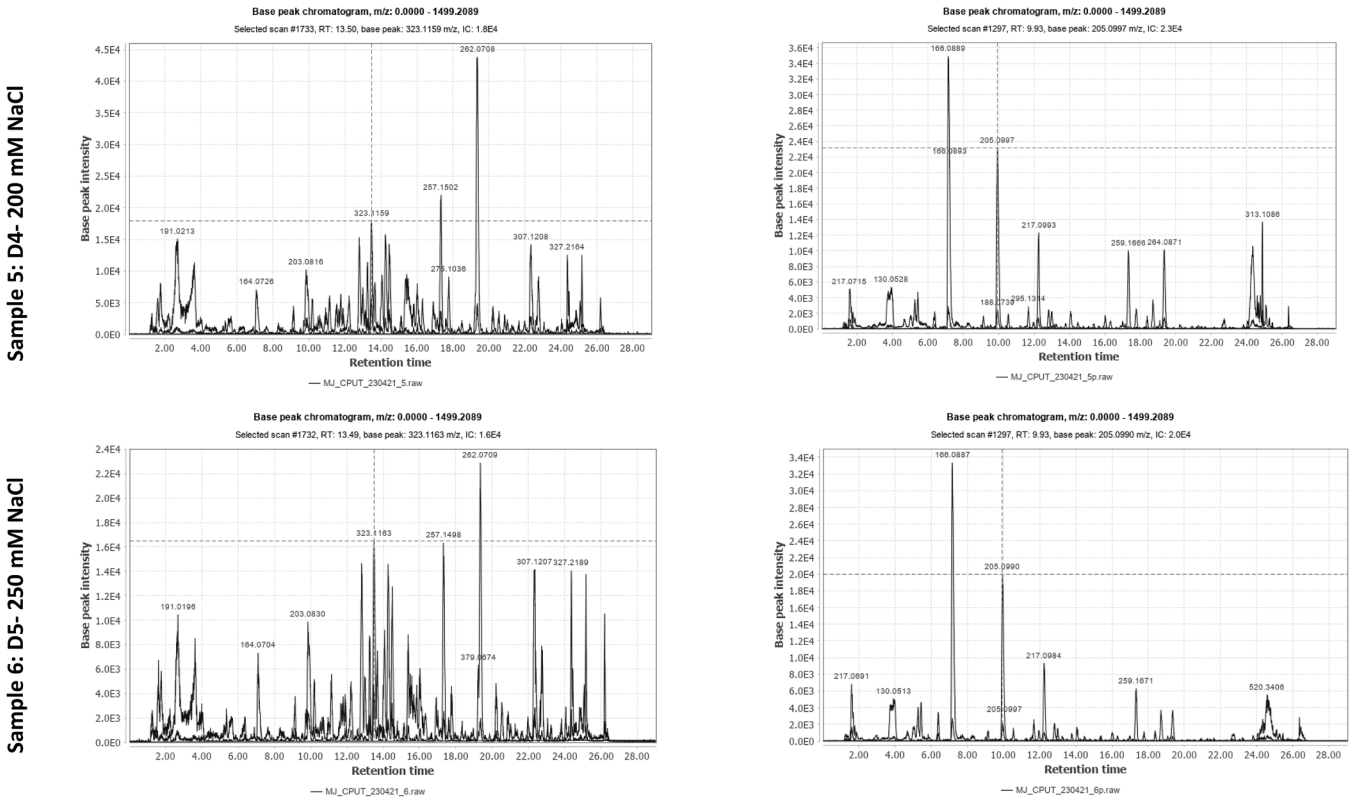

Fig. 1. (*continued*).

3. Results

3.1. Profiling of phytochemicals in crude extracts of T. decumbens

3.1.1. Identification of flavonoids

Thirteen monomeric flavan-3-ols were observed and identified (peaks 45, 46, 50, 51, 54, 56, 59, 62, 64, 70, 75, 76 and 77) (Fig. 1). Stereoisomers: catechin and epicatechin were the basis of identification (Table 1). The order of hydrophobicity for flavan-3ol monomers in the reversed-phase liquid chromatography, i.e. (-/+)-epicatechin > (-/+)-catechin > (-/+)-epigallocatechin > (-/+)- gallocatechin, also enabled identification of the monomers and the oligomers. The order of elution from the column is in the opposite direction. Consequently, it was possible to identify (-/+)-gallocatechin (peak 11) and (-/+)-epicatechin (peak 17). When their precursor ions [M -H]-collision induced dissociation (CID) occurs, catechin and epicatechin often show fragments *m/z* 151, 135 (owing to retro Diels-Alder (rDA) fragmentation); *m/z* 289 (mzCloud). The fragment ions *m/z* 245 ([epicatechin -H-44]-, loss of CO_2), *m/z* 205 ([epicatechin -H-84]-, loss of flavonoid A ring), and *m/z* 179 ([M-H-110]-, loss of flavonoid B ring) are also present.

3.1.2. Identification of flavonols

Peak 73 with MS^1 ion *m/z* 615.1926 was tentatively identified as quercetin 3-O-β-d-(6^{11}-galloyl) galactopyranoside. Quercetin galactoside showed an ion at *m/z* 463 and then MS^2 fragments *m/z* 300, signifying loss of a sugar moiety (−162); fragment *m/z* 300 [M -H-glc]$^-$. Additional acylation of quercetin galactoside with a galloyl group could result in quercetin-3-O-β-d-(6^{11}-galloyl) glucopyranoside. Peaks 81 and 84 were identified as isorhamnetin 3-O-coumaryl rutinoside-7 O-rhamnoside and isorhamnetin 3 O-coumaryl derivative, respectively. The precursor ion *m/z* 843.2032 was due to loss of 72 Da. The fragment ion with an *m/z* of 72 in negative ion mode is a characteristic ring fragment of a (1→6)-linked "anhydro" galactose-H_2O, which lost a (1→3)-branch. The fragment ion for isorhamnetin 3-O-coumaryl rutinoside-7-O-rhamnoside implied 435 [M-H-isorhmatin-coumaryl]-, 675 [M-H-239]-, 239 [M-H-675]$^-$, 299 [isorhamnetin-CH_3]- or 299 [M-H- isorhamnetin-rutinoside-rhamnoside]$^-$. The ion *m/z* 675 was due to the loss of two rhamnosides. Peak 85 was identified as isorhamnetin-O-glucurunoside with *m/z* 494.3253 with MS^2 fragment *m/z* 316 [isorhamnetin-H]$^-$, *m/z* 298 [isorhamnetin-H-CH_3]$^-$, while peak 82 was aglycone isorhamnetin 298 [isorhamnetin+*H*—CH_3]$^+$, 275[M + H—CH_3–CO]$^+$.

3.1.3. Identification of amino acids

Peaks 1, 12, 13, 14, 15, 16, 18, 27 and 55 (Fig. 1) were identified as amino acids. Amino acids were identified following the abundance of protonated ion fragments and derivatives, which could indicate a loss of water (−18 Da), generating their residue mass or loss of (H_2O + CO) to give their immonium ions (−46 Da) (Rogalewicz et al., 2000, Piraudi et al., 2003). Peak 16 was identified as tyrosine, based on a molecular ion peak [*M* + H]$^+$ at *m/z* 182.0847 (calcd 182.0812) and a fragment ion at *m/z* 165[M + H- NH_3]+. Peak 27 was identified in both positive and negative ion modes as tryptophan, based on a protonated molecular ion peak [*M* + H]$^+$ at *m/z* 205.0995 (calcd for 205.0972). Additionally, its MS/MS spectrum displayed a fragment ion [*M* + H- NH_3]$^+$ at *m/z* 188. Notably, this is a preferential loss of ammonia (NH_3) from the protonated tryptophan and is generally shown as a fragmentation pattern, generating the diagnostic 2-carboxyspiro[cyclopropane-indolium] fragment ion. Its derivative was identified in compounds 16 and 55. N-alpha-acetyl-l-ornithine was detected in peak 1 with [ornithine +*H*]$^+$ at *m/z* 133 due to loss of 42 Da of the acetyl group. The ion at 147 was due to loss of CO (28 Da). Peaks 14 and 15 were identified as trans-4-hydroxy-l-proline and cis-4-hydroxy-l-proline, respectively, with characteristic fragment ion of *m/z* 86 due to consecutive loss of water and carbon monoxide (H_2O + CO) [*M* + H- H_2O - CO]$^+$ in accordance with earlier reports (Piraudi et al., 2003). Peaks 12 and 13 were identified as hydroxy-D-proline and a hydroxy-D-proline isomer, respectively, using accurate mass.

Table 1
Phytochemical compounds identified from *T. decumbens*.

No	t_R (min)	$UV_{\lambda max}$ (nm)	*m/z* $(M-H)^-$ / $(M+H)^+$	MS/MS	Tentative identification	Class	Sample
1	1.58	298	175.1221*	147, 133, 156	N-alpha-Acetyl-l-ornithine	Amino acid	D0
2	1.58	299	195.0510	165, 147	Trihydroxycoumarin	Coumarin	D0
3	1.60		229.0500	195, 165, 146	Trihydroxycoumarin derivative	Coumarin derivative	D1, D2, D3, D4, D5
4	1.60	273	195.0910*	127, 166	Caffeine	Alkaloid	D0
5	1.60		217.0695^{*Na}	195, 212, 148, 127	Caffeine	Alkaloid	D1, D2, D3
6	1.72	267	189.0041	133	Catechol sulphate	Phenylsulfate	D0, D1, D2, D3
7	1.77	264	138.0585*	127	Trigonelline	Alkaloid	D0, D1, D3
8	2.21		133.0131	71	Malic acid	Organic acid	D2, D3, D4
9	2.61		191.0206	111, 173	Citric acid	Organic acid	D1, D2, D3, D4, D5
10	2.97	263	136.0666*		Adenine	Nucleoside	D0
11	3.65	285	191.0190	173, 111, 129	Isocitric acid	Organic acid	D1, D2, D3, D4, D5
12	3.66		130.0527*		Hydroxy-d-proline	Amino acid	D0, D1, D2, D3
13	3.95	284	130.0536*		Hydroxy-d-proline isomer	Amino acid	D0, D1, D2, D3
14	4.62	258	132.1053*	86	Trans-4-Hydroxy-l-proline	Amino acid	D0, D1, D2, D3
15	5.05		132.1053*	86	Cis-4-Hydroxy-l-proline	Amino acid	D0, D1, D2, D3
16	5.20	267	182.0847*	165, 136, 153	Tyrosine	Amino acid	D0, D1, D2, D3
17	5.35	265	243.0592	194, 201	(E)-Piceatannol	Stilbenoid	D4, D5
18	5.43	264	196.1015*	150, 165	N'-Formylkynurenine/	Amino acid derivative	D0, D1, D2, D3
	5.45	274	194.0805	161, 128	N'-Formylkynurenine	Amino acid derivative	D0
19	5.58		161.0443	147, 134	Cinnamic acid methyl ester	Benzoic acid ester	D2, D3, D4, D5
20	6.39		282.0841	150, 204	Guanosine	Nucleoside	D1, D2, D3
	6.40	252	284.1026*	152, 149	Guanosine	Nucleoside	D0, D1, D2, D3
21	7.10	257	164.0706	147, 122	Phenylalanine	Amino acid	D1, D2, D3, D4, D5
	7.17	257	166.0881*	120	Phenylalanine	Amino acid	D0, D1, D2, D3
22	9.10		273.1465	175, 184	5,2′-O-dimethyluridine	Nucleotide	D3
23	9.13	273	323.1161	273, 184, 213, 97, 175	Uridine-5′-monophosphate	Nucleotide	D0, D1, D2, D4, D5
24	9.14		275.1622*	234	5,2′-O-dimethyluridine isomer	Nucleotide	D0, D1, D2, D3
25	9.52		273.1451	161, 201	5,2′-O-dimethyluridine isomer	Nucleotide	D3
26	9.75	275	323.1158	204, 119	Coumaric-O-disulfate	Hydroxycinnamic acid derivative	D3
27	9.85	279	203.0809	175	L-Tryptophane	Amino acid	D1, D2, D3, D4, D5
	9.92	279	205.0995*	188	L-Tryptophane	Amino acid	D0, D1, D2
28	10.12	279	321.1013/ 323.1281		digallate	Hydroxybenzoic acid derivative	D0
29	10.20		323.1312		8-Gingerol	Hydroxybenzoic acid derivative	D1, D2, D3, D4, D5
30	10.53	280	252.0886^{-2H}	201, 234, 232	N-oleoylsphingenine	Ceramide	D1, D2, D3
	10.53	279	254.1043*		N-oleoylsphingenine	Ceramide	D0, D1, D2
31	10.59	274	325.1312 340.1311	252, 232	DL—Corydine	Alkaloid	D0, D1, D2, D3
32	10.76	274	193.0363	193	β-d-Glucopyranuronic acid	Saccharide	D0, D1, D3, D4, D5
33	11.13	279	175.0363	115, 113, 136	2-Isopropylmalic acid	Organic acid	D1, D2, D3, D4, D5
34	11.35		193.0363	175, 138	Zingiberone	Hydroxybenzoic acid derivative	D1, D2, D3, D4
35	11.66	272	293.1149	193	6-Gingerol	Hydroxybenzoic acid derivative	D1, D2, D3, D4, D5
	11.69		295.1290*	166, 270, 283	6-Gingerol	Hydroxybenzoic acid derivative	D0, D1, D2, D3
36	11.76	272	425.0770	327, 293	6-Gingerol-o- pentose	Hydroxybenzoic acid derivative	D1, D2, D3, D4, D5
37	11.87	270	307.0823	293, 249	Methyl-6-gingerol	Hydroxybenzoic acid derivative	D1, D2, D3, D4, D5
38	11.97		217.1557*	200, 147, 177, 111, 88	Xanthotoxin	Coumarin	D1, D2, D3, D4, D5
	12.26	270	215.0833	192	Xanthotoxin	Coumarin	D1, D2, D3, D4, D5
39	12.27	270	217.0993*	144, 130	Bergapten	Coumarin	D0, D1, D2, D3
40	12.55	263sh	349.0585	97, 148	N-Coumaroyl-L-tryptophan	Alkaloid	D0, D1
41	12.81	272sh	236.0555		Culmorin	Sesquiterpenoid	D1, D2, D3, D4, D5
	12.81	272	238.0726*	105	Culmorin	Sesquiterpenoid	D0, D1
42	12.99	280	259.0713	215	Meranzin	Coumarin	D1, D2, D3, D4, D5
	12.98	281	261.0875*	188, 217, 145	Meranzin	Coumarin	D0, D1, D2

(*continued on next page*)

Table 1 (*continued*)

No	t_R (min)	$UV_{\lambda max}$ (nm)	*m/z* $(M-H)^-$ / $(M+H)^+$	MS/MS	Tentative identification	Class	Sample
43	13.25	286sh	561.2178$^{[M-2HM-}$	323, 214, 157	Medioresinol-C- gluconide	Lignan	D0, D1, D2, D3, D4, D5
44	13.28		189.1278*	163, 145	Hydroxycoumarin derivative	Coumarin	D1, D2
45	13.41	281	323.1151$^{+H2^{\circ}}$	97	(-/+) Gallocatechin	Flavan-3-ol	D1, D2, D3, D4, D5
46	13.64	281	307.1218^{-2H}	192, 203, 279	(-/-) Gallocatechin	Flavan-3-ol	D1, D2, D3, D4, D5
47	13.97	284sh	337.0935	250, 132, 97, 88	2′-Deoxyadenosine monohydrate	Nucleoside	D0, D1
48	14.05	278sh	250.0714	132, 97	2′-Deoxyadenosine monohydrate	Nucleoside	D1, D2, D3, D4, D5
	14.05		252.0878*	134, 234, 204	2′-Deoxyadenosine monohydrate	Nucleoside	D0, D1, D2, D3
49	14.21		321.1002	241, 97	Digallate	Hydroxybenzoic Acid derivative	D1, D2, D3, D4, D5
50	14.45	280	307.1194	280, 275, 262	(-/+) (*epi*)Gallocatechin	Flavan-3-ol	D1, D2, D3, D4, D5
	14.46		282.0981*	236, 193	(-/+) (*epi*)Gallocatechin metabolite	Flavan-3-ol	D0
51	15.08	270	305.1060	234, 273	(-/-) (*epi*)Gallocatechin	Flavan-3-ol	D0, D1, D2, D3
52	15.21	267	185.0385	97	2,5-Dimethylbenzene–sulfonic acid	Benzene derivatives	D0, D3, D4, D5
53	15.37		371.0952$^{[2M-H]-}$	185, 264	2,5-Dimethylbenzene–sulfonic acid dimer	Benzene derivatives	D2, D3, D4, D5
54	15.80	281	305.1073	97, 203	(-/+) (Epi)gallocatechin	Flavan-3-ol	D0, D1, D2, D4, D5
55	16.01		252.0893*	206	3-Hydroxy-DL-kynurenine	Amino acid derivative	D1, D2
	16.02		206.0818$_2^{[M-H-H]}$	164	3-Hydroxy-DL-kynurenine	Amino acid derivative	D1, D2, D3, D4, D5
56	16.16		305.1041	97, 241	(-/-) (Epi)gallocatechin	Flavan-3-ol	D0, D3, D4, D5
57	16.30	309	280.0804	163, 262, 244	N-cis-Coumaroyl-tyramine	Alkaloid	D0, D1, D2, D4, D5
	16.33	309	282.0966*	264, 136, 165, 207	N-cis-Coumaroyl-tyramine	Alkaloid	D0, D1, D2
58	16.89		291.0898	206, 97, 279	(-/+) Catechin	Flava-3-ol	D0, D1, D2, D4, D5
59	16.96	311	266.1017* $[M+2H+Na]2+$ (288.0789)	248, 166, 208, 120	(-/+) Catechin	Flavan-3-ol	D0, D1, D2
60	17.32		259.1665*	197, 84	Not identified	–	D0, D1, D2, D3
	17.34	318	257.1502	215, 197			D1, D2, D4, D5
61	17.62		403.1593	223, 97, 321	Uridine-5′-diphosphate	Nucleotide	D2, D3
62	17.77	283	275.1046	245, 193	Unidentified flavanol metabolite	Flavan-3-ol	D4, D5
63	17.79		289.0802	245, 275, 193	(-/-) Catechin	Flavan-3-ol	D2
64	18.33		413.1462	269, 349, 183, 125, 59	Catechin benzoyl ester	Flavan-3-ol	D1, D3
65	18.42	278, 312	355.1996*	149	Ferulic acid glucoside	Hydroxycinnamic acid derivative	D0, D1, D3
66	18.79	279, 312	197.1191*	162, 179	Dihydroferulic acid	Hydroxycinnamic acid derivative	D0, D1, D2, D3
67	18.95	264, 312	279.1244	258, 269, 144	Coumaroyl malate	Hydroxycinnamic acid derivative	D1, D3
68	19.26	325sh	379.0658	262	Diacetoxy-6-gingerdiol	Hydroxybenzoic acid derivative	D1, D2, D4, D5
69	19.35	279	262.0728^{-2H}	146, 218	Abscisic acid	Carotene derivative (terpenoids)	D1, D2, D3, D4, D5
	19.36	278	264.0886*	131	Abscisic acid	Carotene derivative (terpenoids)	D0, D1, D2, D3
70	20.20	275, 317	291.1267^{-2H}	207, 165, 147	(-/+) Epicatechin	Flavan-3-ol	D1, D2, D3, D4, D5
71	20.56	281, 312	187.0990	169, 125	Gallic acid monohydrate	Hydroxybenzoic acid derivative	D0, D1, D3, D4, D5
72	20.87	311	429.1724	335, 89, 205, 119, 249, 317	1,3-O-Feruloyl-caffeoylglycerol	Hydroxycinnamic acid derivative	D1, D2, D3, D4, D5
73	21.04	276, 323	615.1926	463, 464, 300, 445, 405, 289	Quercetin 3-O-*β*-d-(611-galloyl) galactopyranoside	Flavonol	D2, D4, D5
74	21.28	272, 324	837.3243	691, 335, 417, 477, 245, 805, 191, 162	Caffeoyl shikimic acid-O-sulphate dimer	Hydroxycinnamic acid derivative	D0, D5
	21.30	273, 319	839.3311*	693, 337, 211	Caffeoyl shikimic acid-O-sulphate dimer	Hydroxycinnamic acid derivative	D0
75	21.67	278, 332	637.1368	289, 305, 573, 403, 203	(Epi) gallocatechin-3-O-(6^{11}-O-gallate) glucoside	Flavan-3-ol	D3
76	21.96		289.1105	245	(-/-) Epicatechin	Flavan-3-ol	D1, D2, D3, D4, D5
77	22.25	281, 316	307.1208	97	(-/-) (Epi)gallocatechin	Flavan-3-ol	D1, D2, D3, D4, D5
78	22.74	324	209.0821*	191, 161, 193	Sinapaldehyde	Hydroxycinnamic acid derivative	D0, D1, D2
79	22.76	324sh	393.0822$^{[M-Na-2H]-}$	243, 185	Sinapaldehyde-4-O-beta-d-glucopyranoside	Hydroxycinnamic acid derivative	D1, D2, D3, D4, D5
80	23.06	281, 329	915.1870$^{[M-2H]-}$	435, 675, 239, 299	Isorhamnetin 3- O -coumaryl rutinoside-7- O -rhamnoside	Flavonol	D4, D5

(*continued on next page*)

Table 1 (*continued*)

No	t_R (min)	$UV_{\lambda max}$ (nm)	*m/z* $(M\text{-}H)^-$/ $(M+H)^+$	MS/MS	Tentative identification	Class	Sample
81	23.26	281, 329	843.2032	299, 161, 343	Isorhamnetin 3- O -coumaryl hexoside derivative	Flavonol	D2, D5
82	24.34		316.2860*	221, 298, 275, 195	Isorhamnetin	Flavonol	D2, D3
83	23.80		312.1224	263, 269	Dihydroxy-octadecenoic acid	Fatty acid	D2, D5
84	24.05	282, 326	813.1809	675, 163	Isorhamnetin 3-O-coumaryl hexoside derivative	Flavonol	D2, D3, D4, D5
85	24.28	284, 313	494.3253	316, 298	Isorhamnetin-O-glucurunoside	Flavonol	D4
86	24.36	284	327.2162	215	Trihydroxy-octadecadienoic acid	Fatty acid	D1, D2, D3, D4, D5
87	24.36	284	316.2854*	316, 298, 293, 221, 275, 195	3-O-methylellagic acid	Tannin	D0, D1
88	24.45	318, 405	329.2289	227, 282	3,3′-di-O-methylellagic acid	Tannin	D1, D2, D3, D4, D5
89	24.57		454.2946*	326, 187, 275	Trihydroxy-octadecadienoic acid derivative	Fatty acid	D2
90	24.59		520.3604*	326, 187, 332	Trihydroxy-octadecadienoic acid derivative	Fatty acid	D5
91	24.79		225.1602*	193, 100, 211, 158	Methyl jasmonate	Lipid	D0, D1, D2, D3, D4
92	24.87		265.1463	145	Decarbonylated hydroxy octadecadienoic acid	Fatty acid	D0, D1, D2, D3, D4, D5
93	24.90	275	313.1062*	225, 306, 275 220	5,7,4′-Trimethoxyflavone	Flavone	D1, D2, D3, D4, D5
94	25.07		293.2092	265, 145	Hydroxy octadecadienoic acid	Fatty acid	D0, D1, D2, D3, D4, D5
95	25.10		326.3033	225, 277	Trihydroxy-octadecadienoic acid isomer	Fatty acid	D2, D4
96	25.17		311.2208	293, 265	Dihydroxyoctadecadienoic acid	Fatty acid	D0, D5 D1, D2, D3, D4, D5
97	26.20		271.2258	265	Hydroxy palmitic acid	Fatty acid	D0, D1, D2, D3, D4, D5
98	26.38		247.1668*	227, 124	Zederone	Sesquiterpene	D1, D2, D3, D4, D5

Results are presented as D0= Control, D1= 50 mM NaCl, D2= 100 mM NaCl, D3= 150 mM NaCl, D4= 200 mM NaCl and D5= 250 mM NaCl.

3.1.4. Identification of alkaloids

Four alkaloids were detected and identified in peaks 4, 7, 21 and 57. The protonated ion of trigonelline exhibited *m/z* 138.0585 $[M+H]^+$ and caffeine, *m/z* 195.0910 $[M+H]^+$ in the positive ion mode, which gave major product ions at *m/z* 120 $[M+H\text{-}H_2O]^+$ and 138 $[M+H$ –O—C –$NCH_3]^+$; (methyl isocyanate, 57 Da), respectively. Peak 21 was identified as phenylalanine, corroborating earlier research (Harnly et al., 2007). Compound 57 was provisionally identified as N-trans--coumaroyl-tyramine in both positive and negative ion modes. The spectrum exhibited [M-H]- at *m/z* 282, with significant MS^2 fragments at *m/z* 119 ([coumaric acid - CO_2]-) and *m/z* 173 ([M-H- coumaric acid - $CO_2]^-$.

3.1.5. Identification of stilbenoids

Piceatannol (*m/z* 243.0592, peak 17) was also identified by a previous report and accurate mass. The MS^2 spectrum produced ions at *m/z* 194 $[M\text{-}H\text{-}8]^-$, arising from the loss of a water molecule, and at *m/z* 201 $[M\text{-}H\text{-}42]^-$ due to loss of C_2H_2O.

3.1.6. Identification of hydroxycinnamic acid derivatives

Eight hydroxybenzoic acids and their derivatives were identified (peaks 26, 65, 66, 67, 72, 74, 78 and 79) (Fig. 1). Most of them could absorb UV at about 325 nm (those with caffeoyl moiety) compounds or 309 nm (with coumaroyl). Compound 26 was identified as coumaroyl disulphate using its accurate mass and fragment ions *m/z* 119, 204. Additionally, a derivative with *m/z* 163 ([coumaric acid-H]-) and an MS^2 fragment at *m/z* 119 ([coumaric acid-CO_2]-) may be produced when coumaric acid is present (Hokkanen et al., 2009). Thus, peak 67 was identified as coumaroyl malate and peak 78 was tentatively identified as sinapaldehyde.

3.1.7. Identification of hydroxybenzoic acid derivatives

Nine hydroxybenzoic acids and their derivatives could be identified (peaks 28, 29, 34, 35, 36, 37, 49, 67 and 71). Their UV absorption maxima range between 270 and 282 nm. In the negative ion mode, the quasi-molecular ion $[M\text{-}H]^-$ of the compound with *m/z* 293.1149 belonged to that of beta-hydroxy ketones, 6-gingerol. According to the information of the high-resolution accurate mass, fragment ions at *m/z* 193.0856 were identified in the cleavage between C6 and C7 bonds of such a compound (Jiang et al., 2005). Gingerol pyrolysis produces zingiberone with *m/z* 193.0363 and its main fragment 175([M-H-H_2O]-). Gingerols in positive ion mode can show protonated molecular ions ($[M+H]^+$), H_2O subtracted protonated molecular ions ($[M\text{-}H_2O+H]^+$). Compounds 29 and 35 were identified as 8-gingerol and 6-gingerol, respectively. Fragment ions were 275 ($[M\text{-}H_2O—H]^-$), and 305 ($[M\text{-}H_2O—H]^-$), or 277 ($[M\text{-}H_2O—CH_3—H]^-$ for methyl-6-gingerol are common (Park and Jung, 2016). The MS^1 ions were *m/z* 293 and 321, respectively, producing common fragment ion *m/z* 113 $[C_7H_{13}O]^-$in MS^2 formed as a result of inductive cleavage of the side chain. The ion fragment at *m/z* 137 was due to the cleavage of an alkyl chain with its acetoxy group. The formation of fragment ions at *m/z* 321, [M-H-AcOH]-, suggests a di-acetylated derivative of 6-gingerdiol; thus compound 67 was identified as diacetoxy-6-gingerdiol (Jolad et al., 2004). Compound 36, with some similarity in fragmentation in its pattern, showed an increase of pentose sugar (28 Da), thus identified as 6-gingerol pentose. Methyl gingerol showed precursor ion at *m/z* 307.0823 after addition of 15 Da on 293 and fragment 249 [gingerol-H-$CO_2]^-$. Compound 87 was identified as gallic acid monohydrate with *m/z* 187.0990 and fragments 169 [gallic acid-H]-, and [gallic acid-$H_2O—CO_2]^-$. A digallate could be identified at 321.1002 $[M\text{-}H]^-$.

3.1.8. Identification of tannins

Peaks 89 and 90 were identified as 3-o-methyl ellagic acid and 3,3′-di-o-methyl ellagic acid, respectively, owing to absorptions at 405 nm and typical fragments in MS^2 spectra (*m/z* 316, 298, 227, 275, 195) (Kramberger et al., 2020). The fragments were identified as: 316 $[M+H—CH_3]^+$, 298 $[M\text{-}H\text{–}OCH_3]^-$, 282 $[M\text{-}CO—H_2O]$, 242 $[M\text{-}H\text{-}2CO_2]$- and 227 $[M\text{-}2CO_2\text{–}OH+2H]^+$. The fragments indicate the loss of the

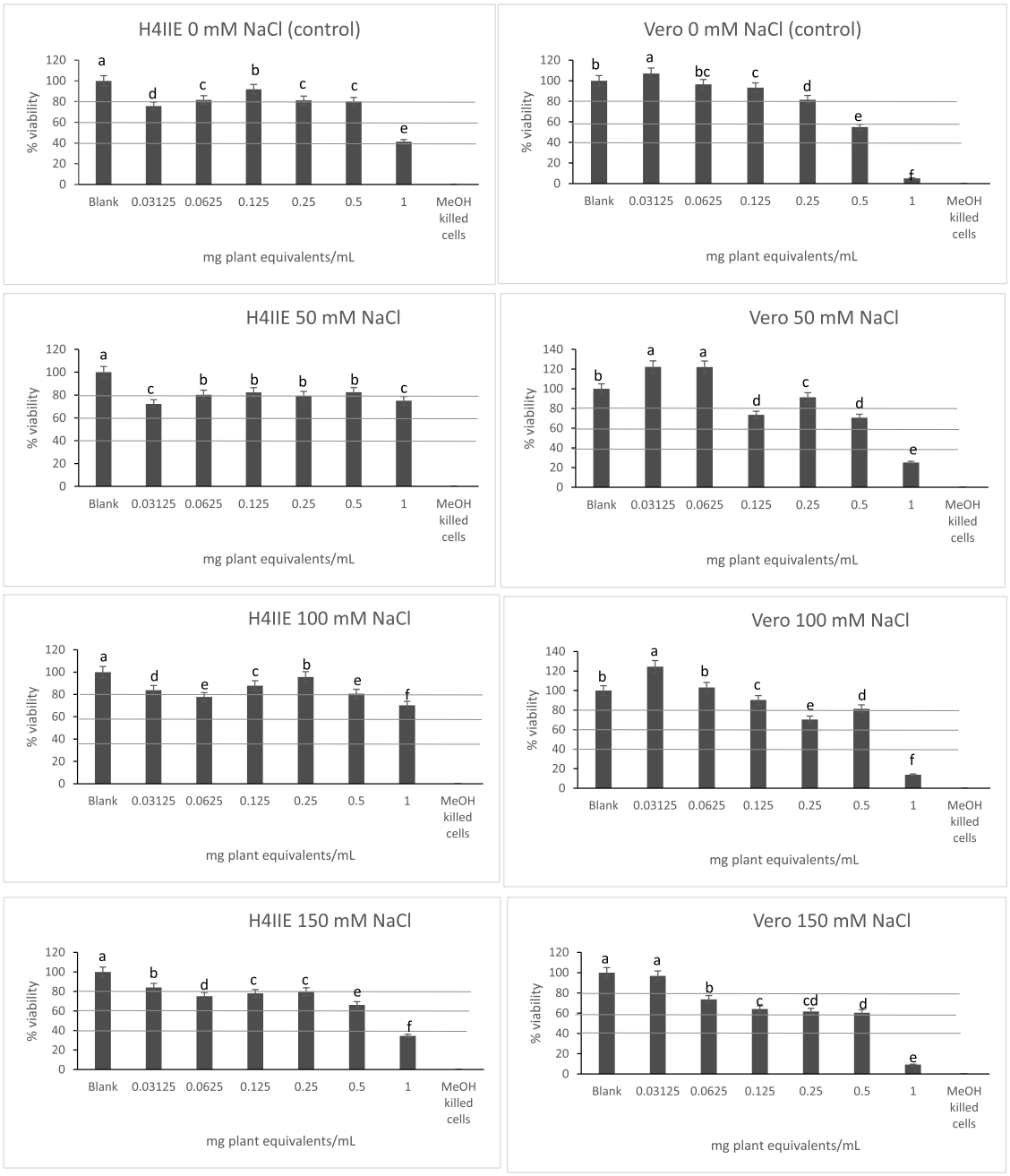

Fig. 2. Cytotoxicity of *T. decumbens* crude extract against cancerous (H4IIE) and non-cancerous (Vero) cells. The bar graph illustrates the triplicate values of the experiment. Different letters indicate statistical significant differences between treatments ($p < 0.05$). Anti-inflammatory activity.

methyl [M-H-15]-, methoxy $[M\text{-}H\text{-}31]^-$, carbonyl (acylium ion) $[M\text{-}H\text{-}28]^-$, and carbon dioxide [M-44] moieties from the compound.

3.1.9. Identification of coumarin

Coumarins and furanocoumarins were detected at peaks 2, 3, 38, 42, and 44 (Fig. 1). Most of the peaks exhibited UV λ max at 274 nm, characteristic of coumarin. Peak 38 was identified as xanthotoxin (hydroxyl psoralen) with an MS^2 ion *m/z* 192 $[M + H—CO]^+$ and 175 $[M + H—CO_2]^+$. The $[M + H]^+$ ion was shown at *m/z* 232. The fragment at *m/z* 188 was formed from the RDA cleavage of the furano ring, losing the C_2H_2O-fragment ion. Peak 42 was identified to be merazin, as was identified in previously.

3.1.10. Identification of organic and fatty acids

The spectra of fatty acid compounds displayed abundant ions due to the loss of CH_2, CO_2, and H_2O groups. Some derivatives of linoleic acid methyl jasmonate with MS^1 ion at *m/z* 225.1602 MS^2 fragment *m/z* 193, perhaps due to loss of CH_3O (−32 Da). Ten fatty acids were characterised (peaks 83, 86, 89, 90, 91, 92, 94, 95, 96, and 97). Polyunsaturated and hydroxylated fatty acids were identified as compounds. Hydroxylated fatty acids showed an extra loss of water molecules. The hydroxy decenoic acid fragment showed at 187 in positive ion mode and at 185 Da in negative ion mode. The polyunsaturated fatty acids included dihydroxydecanoic acid at peaks of 83, 86, 95 and 96, dihydroxy-octadecenoic acid (*m/z* 312.1224) and trihydroxyoctadecadienoic acid (*m/z* 327.2162). Trihydroxyoctadecanoic acid showed main MS/MS fragments at *m/z* 311 and 293 due to the

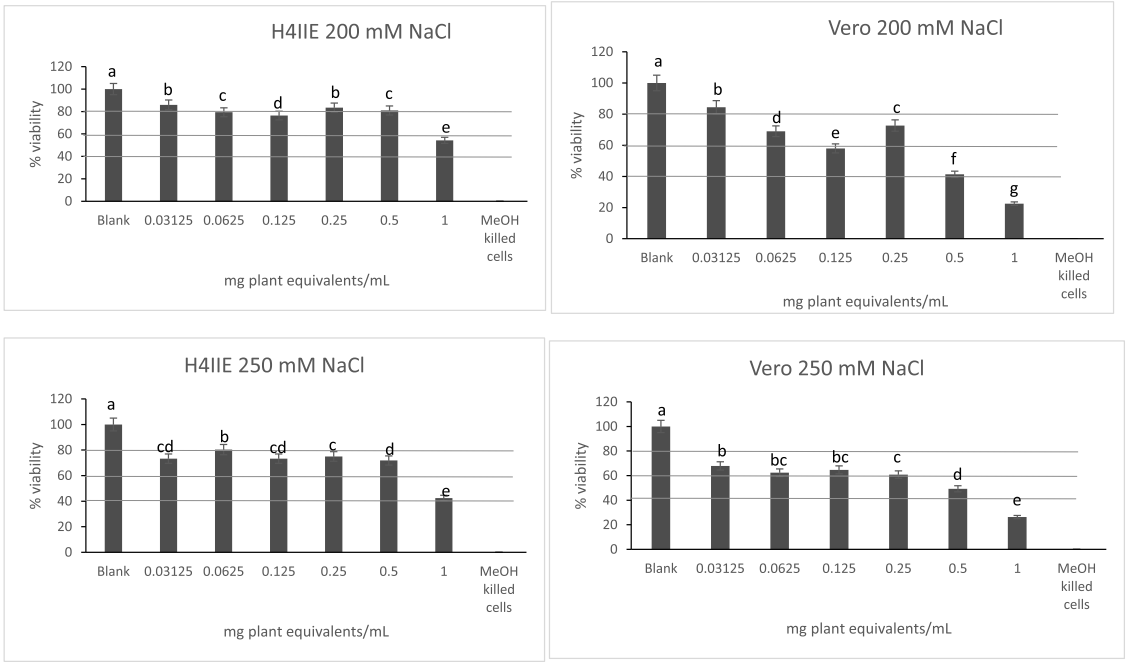

Fig. 2. (*continued*).

subsequent loss of two water molecules and the main fragment at *m/z* 211 due to the C15/C16 bond cleavage. Additionally, dihydroxy-octadecadienoic acid was identified at peak 96. LC-MS also revealed monohydroxy-fatty acid, hydroxy octadecadienoic acid with *m/z* 293.2092 at peak 94, saturated fatty acid, hydroxy palmitic acid was also identified at peaks 97, and this is in agreement with previous work (Ibrahim et al., 2023).

3.1.11. *Identification of nucleoside/nucleotide*

These included adenosine, cytidine, guanosine, and uridine. Nucleosides, such as guanosine involve neutral losses of CO, NH_3, CH_2CH_2, $NHCH_2$, NHCO, and NH_2CN and glycosidic C–N bond cleavage. Fragment ions *m/z* 282, *m/z* 284 correspond to the deprotonated/protonated molecular ions of guanosine, and ions *m/z* 150, *m/z* 152 are deprotonated and protonated forms of guanine (Table 1).. The ion *m/z* 150 or *m/z* 152 was due to glycosidic C–N bond cleavage after losing 132 Da of sugar moiety along with its respective nucleoside (Liu et al., 2008). 2′-Deoxyadenosine monohydrate (peak 47, *m/z* 337.0935 $[M\text{-}H]^-$) also involves this kind of rupture as the only option (Flosadóttir et al., 2011). Pyrimidine nucleosides included uridine-5′-monophosphate (peak 23) and uridine-5′-diphosphate (peak 61), identified with precursor ion *m/z* 323.1161 and 403.1593, respectively. Its methyl derivative, 5,2′-O-dimethyluridine, showed ion *m/z* 273.1465. Pyrimidine nucleosides can use two channels of fragmentation: glycosidic C–N bond cleavage and base fragmentation leading to the formation of NCO- and $[M\text{–}H\text{–}HNCO]^-$ (Flosadóttir et al., 2011). The MS^2 fragment ions consisted of 97 $[PO_4]^{2-}$, 184 $[M\text{-}C_2H_4O_2]^-$ (0.3X sugar cross ring cleavage), 175 $[M\text{-}C_3H_4N_2]^-$ (base fragmentation). Phosphoribose-derived signals included *m/z* 213 for ribonucleotide phosphate RbP.

The cytotoxicity effect of ethanolic extracts of *T. decumbens* was examined on cancerous (H4IIE-*luc*) and non-cancerous (Vero) cells for potential use in cancer therapy. The viability of cells was measured with the MTT viability assay using the ISO 10,993 template, where viability of >80 % = non-cytotoxic, 60–80 % = weak cytotoxic, 40–60 % = moderate cytotoxic and viability of <40 % = strong cytotoxic. Tested cells were treated with extracts at various dosages (0.03, 0.06, 0.13, 0.25, 0.5 and 1 mg/mL) for 24 h. The results showed that the crude extracts of saline treatments (0–250 mM NaCl) at dosages of 0.03, 0.06, 0.13, 0.25, and 0.5 mg/mL had a weaker cytotoxicity against cancerous cells, while the largest dose (1 mg/mL) from 150 mM treatment showed a stronger cytotoxicity (Fig. 2). Nonetheless, this concentration (1 mg/mL) also showed a stronger cytotoxicity against non-cancerous cells. These results demonstrate that the crude extracts of *T. decumbens* possess a weaker anti-cancer potential in most concentrations except for 1 mg/mL. However, this concentration is toxic to non-cancerous cells as well, thus it is not recommended for use.

The crude extracts exhibited significant anti-inflammatory efficacy, which was demonstrated the reduction in nitrite concentration in lipopolysaccharide-stimulated RAW macrophages, without impacting cell survival (Fig. 3). Cells without LPS activation served as negative control, while LPS-induced cells treated with aminoguanidine (AG) served as positive control. Results revealed a significant reduction in nitrite concentration in LPS-induced cells treated with a dose of 100 μg/mL of the crude extract derived from 100 mM NaCl treatment. This dosage had a lower nitrite concentration compared to other LPS-induced cells, including the positive control. Additionally, this dosage maintained a cell viability of over 80 %, thus showcasing a safe and potent anti-inflammatory activity.

3.2. *Acetylcholinesterase (AChE) activity*

Salinity stress significantly influenced the acetylcholinesterase (AChE) inhibitory activity of *T. decumbens* extracts on H4IIE-*luc* cells (Fig. 4). The results indicate that all crude extracts derived from salt treatments had a notable inhibitory effect on AChE activity in H4IIE-*luc* cells. Extracts derived from the control (0 mM NaCl) treatment had significantly ($p < 0.05$) greater inhibition of AChE activity, followed by 50 and 100 mM NaCl, respectively, compared to the untreated cells.

4. Discussion

Edible halophytes have recently gained popularity as a source of food with functional capabilities due to their nutritional constituents and the presence of medicinal compounds (Sogoni et al., 2025). These species have been reported to produce novel bioactive compounds under salinity stress and are used in the management of various ailments in humans due to their therapeutic potential (El-Saadony et al., 2023; Mohammed et al., 2023). In this study, UHPLC-MS analysis identified 98

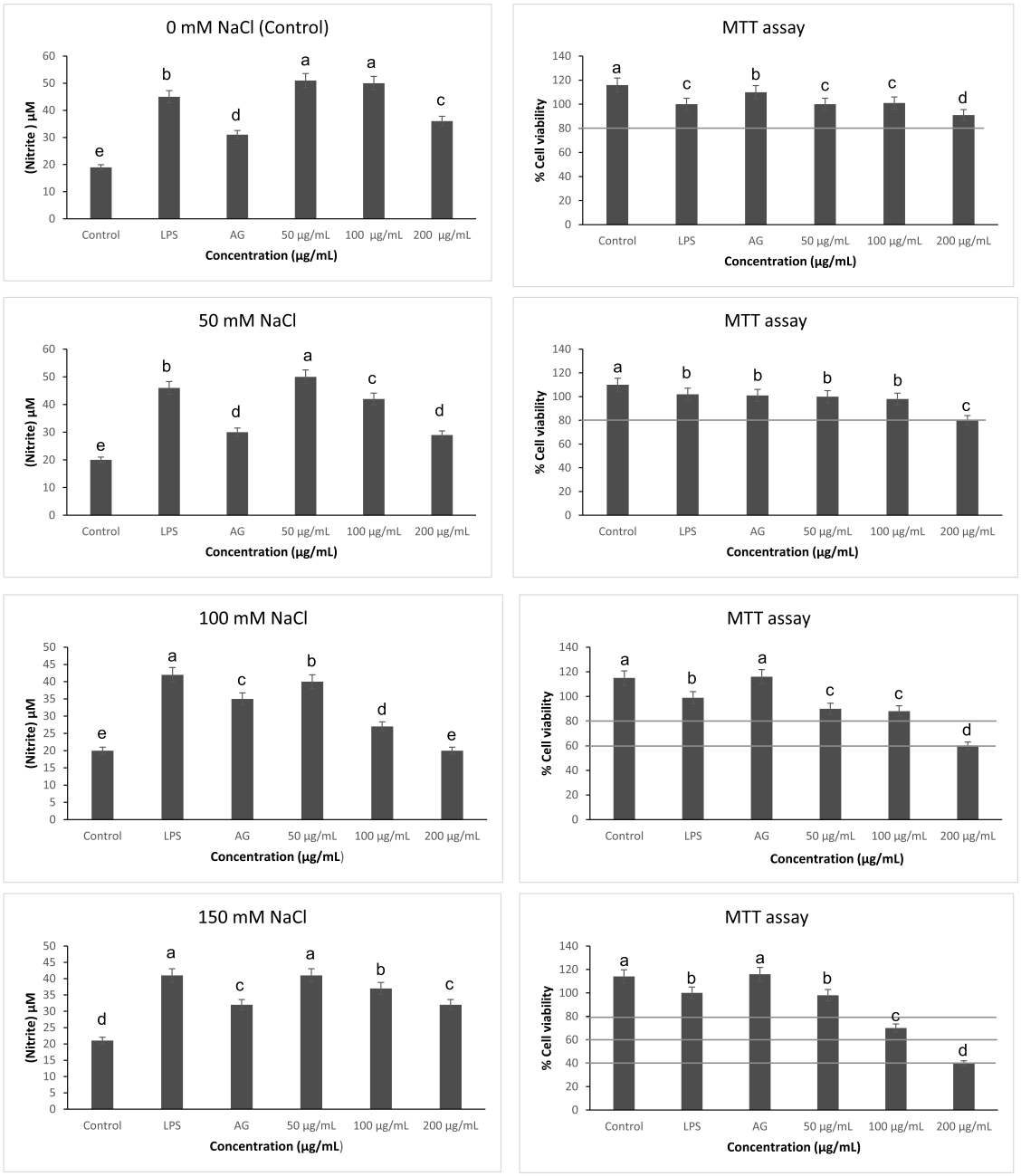

Fig. 3. Nitric oxide production and cell viability (%) of LPS-stimulated macrophages after 24-hour exposure to treatments. The bar graph illustrates the quadruple values of the experiment. Different letters indicate statistical significant differences between treatments ($p < 0.05$).

compounds in *T. decumbens* for the first time, most of which were flavonols, stilbenoids, hydroxybenzoic acid derivatives, alkaloids, coumarin, and hydroxycinnamic acids among others. These compounds are known to exert various biological activities ranging from cardio-protection, neuroprotection, anti-cancer, anti-diabetic properties, antimicrobial and anti-inflammation among others.

Cancer ranks among the most prevalent causes of mortality globally, with an accelerating death rate particularly evident in developing nations (Soerjomataram et al., 2023). Thus, drawing attention to an affordable and effective anticancer treatment. Plant-based medicine of natural origin with enhanced metabolites has been recently recommended as anti-cancer adjuvant therapies due to their anti-proliferative and pro-apoptotic properties (Chimento et al., 2023).

Anticancer activity of plant-based compounds has been extensively documented in the literature (Bhattarai et al., 2021; Maheshwari and Sharma, 2023). For instance, hydroxycinnamic acids have been reported to increase the cytotoxicity and apoptosis of DU145 prostate cancer cells (M.O. Jimoh et al., 2024). Sesquiterpene also showed good inhibition of cancer cells (HeLa and MCF-7) (Shoaib et al., 2017), while stilbenes have been reported to block the metabolic activation of pro-carcinogens by inhibiting specific isoforms of cytochrome P450 (CYP) enzymes and thus preventing the initiation of carcinogenesis in cultured human tumour cells (Akinwumi et al., 2018). Interestingly, prominent anti-cancer compounds such as stilbenoid ((E)-Piceatannol) (Piotrowska et al., 2012), hydroxybenzoic acid derivatives (6-gingerol and 6-gingerol-o-pentose) (Salari et al., 2023), tannin (3,3′-di-O-methyl ellagic acid) (Harper, 2023) and coumarins (Bergapten and Xanthotoxin) (Mirzaei et al., 2017) were identified in *T. decumbens.* Nonetheless, the ethanolic

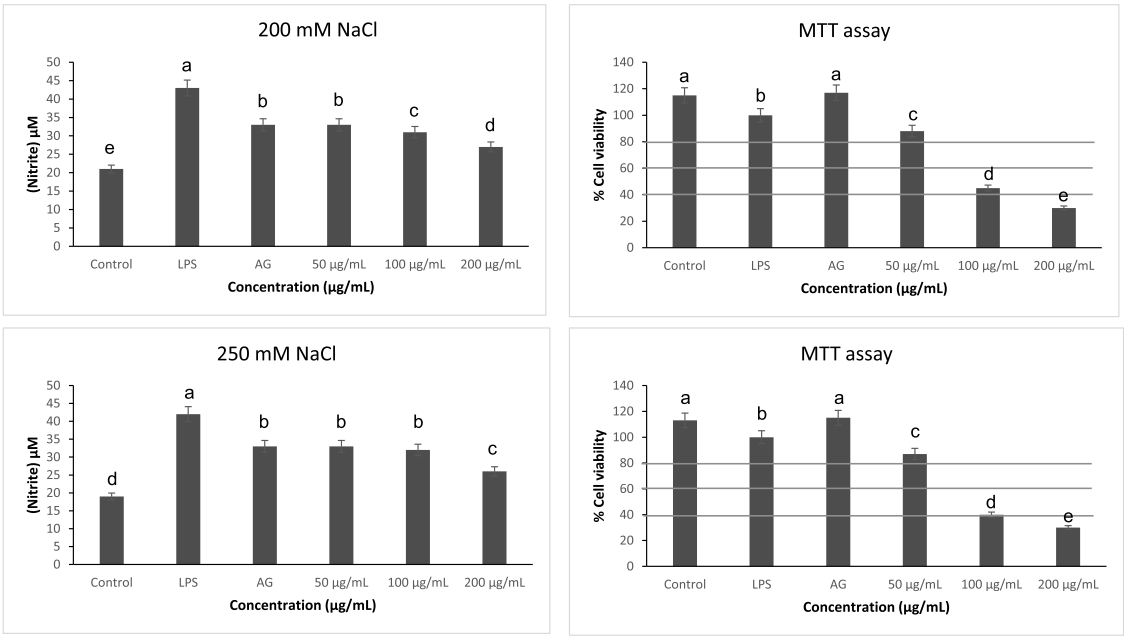

Fig. 3. (*continued*).

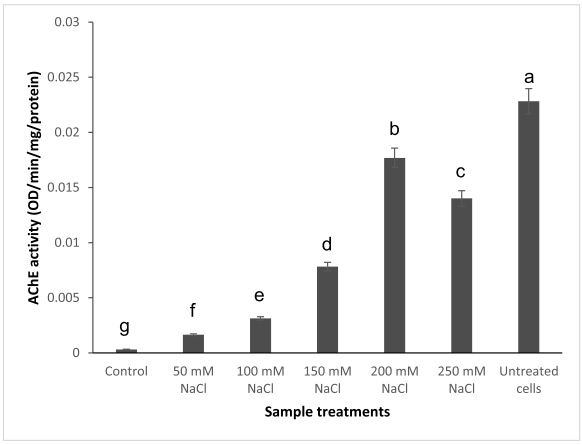

Fig. 4. Acetylcholinesterase inhibitory potential of *T. decumbens* extracts. Different letters indicate statistically significant differences between treatments ($p < 0.05$).

extracts possessed mild anti-cancer potential against H4IIE-luc (cancerous rat hepatoma) in most concentrations but showed a stronger cytotoxicity at the dosage of 1 mg/mL on both cancer and non-cancer cells. This may be due to synergistic and antagonistic effect of heterogenous metabolites in this species or the compounds could have exhibited broad spectrum toxicity, thereby causing non-specificity to cancerous and non-cancerous cells. Thus, future research on the isolation of these compounds becomes imperative to underpin their toxic concentrations against cancer cells.

Inflammation is a biological defence mechanism that enables cells to protect themselves against pathogens and toxins, as well as defective immune regulation (Borquaye et al., 2020). However, unending inflammatory actions result in tissue dysfunction and damage, leading to numerous ailments (Achasih Quinta Nkemzi et al., 2024). Current treatment for inflammation has been accomplished by the use of non-steroidal anti-inflammatory drugs (Gonfa et al., 2023). Nevertheless, adverse consequences linked to the extended use of these anti-inflammatory drugs have created a demand for novel treatments with minimal side effects. Previous studies have uncovered natural anti-inflammatory compounds, such as phenolics and flavonoids, to be beneficial in the treatment of chronic inflammatory diseases associated with overproduction of nitric oxide (Oguntibeju, 2018).

In this study, the anti-inflammatory efficacy of the crude extracts was shown by the reduction in nitrite concentration in lipopolysaccharide-stimulated RAW macrophages, without impacting cell survival. A potent anti-inflammatory activity was observed at the dose of 100 µg/mL crude extract of 100 mM NaCl treatment, and this was significantly greater than cells treated with aminoguanidine (positive control), with no effect on cell viability. The potent anti-inflammatory activity observed when cells were exposed to extract of *T. decumbens* could be due to the presence of identified phenolic-derived compounds such as phenylsulfate (catechol sulphate), sesquiterpene (zederone), hydroxybenzoic acid (6-gingerol-o-pentose) and alkaloid (trigonelline), which are reported to have anti-inflammatory activity (Ha et al., 2017; Khalili et al., 2018; Pintatum et al., 2020; Promdam and Panichayupakaranant, 2022). These results consistent with the findings of F. , who reported a commendable anti-inflammatory activity of the ethanolic leaf extract of *Morinda lucida* and was linked to the presence of phenolic-derived compounds such as alkaloids and flavonoids known for their anti-inflammatory potential. Similarly, Nethengwe et al. (2024) also reported a significant reduction in nitrite concentration in a dose-dependent manner of *Garcinia livingstonei* aqueous extract in LPS-induced cells with no signs of toxicity. Therefore, based on these results, *T. decumbens* could be considered as a potential source of anti-inflammatory treatment.

Alzheimer's disease (AD) is the predominant form of dementia, a progressive age-associated condition marked by the deterioration of brain function (Chauhan et al., 2024). This is attributable to the diminished amounts of the neurotransmitter acetylcholine in the brains of the elderly as the disease advances, leading to a decline in cognitive function (Nguyen et al., 2020; Taqui et al., 2022). The use of plant-based extracts as AChE inhibitors in AD has been reported to enhance acetylcholine levels in the synaptic area, thus reinstating impaired cholinergic neurotransmission (Huang et al., 2022; Prasathkumar et al., 2022). In this study, ethanolic extracts of *T. decumbens* significantly inhibited the AChE activity in H4IIE-*luc* cells with a pronounced effect in 0 and 50 mM NaCl samples compared to untreated cells. This inhibition could be linked to the presence of 3-hydroxy-DL-kynurenine, an amino acid

known to regulate oxidative stress and neurotoxicity in the brain (Liang et al., 2022; Sharma et al., 2022). These findings are in agreement with the study conducted by M. , where *Aegle marmelos* extracts inhibited rat brain AChE. Moreover, the effectiveness of plant-based extracts in inhibiting AChE was also reported by M.J. on several medicinal plants and was attributed to the presence of anticholinesterase compounds. The presence of anticholinesterase compounds in the leaf extracts of *T. decumbens* suggests that this species could be used as a potential AChE inhibitor for the treatment of AD.

5. Conclusions

This study was the first to explore the chemical profile of metabolites aggregated in the crude extracts of *T. decumbens* as well as their cytotoxicity, AChE inhibitory activity, anti-cancer and anti-inflammatory potential. The chemical profile of metabolites revealed the presence of flavonoids, flavonols, stilbenoids, hydroxybenzoic acids, alkaloids, and hydroxycinnamic acids, among others. Moreover, the crude extracts exhibited a potent inhibitory effect on inflammation and AChE, while they had a mild effect on cancer cells. The pharmacological effects displayed by the crude extract of this halophyte could be attributed to the identified medicinal compounds, which indicates its potential as a promising source for isolating pure compounds that could be useful in developing new anti-inflammatory and acetylcholinesterase inhibitor drugs. Therefore, these findings could be beneficial for future research avenues on the application of this species in the formulation of nutraceuticals and pharmaceuticals.

Funding

This work was supported by the National Research Foundation (NRF) of South Africa: Grant number 140847. The conclusions made are those of the authors and are not to be attributed to the NRF.

CRediT authorship contribution statement

Avela Sogoni: Writing – original draft, Methodology, Formal analysis, Data curation, Conceptualization. **Muhali Olaide Jimoh:** Writing – review & editing, Validation, Supervision, Data curation. **Nasifu Kerebba:** Writing – review & editing, Methodology, Formal analysis, Data curation. **Sihle Ngxabi:** Writing – review & editing, Validation, Software, Resources. **John Paul Giesy:** Writing – review & editing, Validation, Methodology. **Rialet Pieters:** Writing – review & editing, Validation, Methodology, Formal analysis. **Suranie Horn:** Writing – review & editing, Validation, Resources, Formal analysis, Data curation. **Learnmore Kambizi:** Writing – review & editing, Validation, Supervision, Funding acquisition, Conceptualization. **Charles Petrus Laubscher:** Writing – review & editing, Validation, Supervision, Project administration, Conceptualization.

Declaration of competing interest

The authors declare that they possess no conflicting interests or personal ties that may have seemingly influenced the work presented in this study.

Acknowledgement

The authors of this work express their gratitude to the North-West University for its technical and laboratory support. JPG was supported by a Distinguished Visiting Professorship in Environmental Sciences at Baylor University in Waco, Texas, USA.

References

Aarts, J.M.M.J.G., Denison, M.S., Haan, L.H.J.de, Schalk, J.A.C., Cox, M.A., Brouwer, A., 1993. Ah-receptor mediated luciferase expression: a tool for monitoring dioxin-like toxicity. Organohalogen Compd. 13, 361–364.

Akinwumi, B.C., Bordun, K.A.M., Anderson, H.D., 2018. Biological activities of stilbenoids. Int. J. Mol. Sci. 19, 792. https://doi.org/10.3390/IJMS19030792.

Anand, U., Dey, A., Chandel, A.K.S., Sanyal, R., Mishra, A., Pandey, D.K., De Falco, V., Upadhyay, A., Kandimalla, R., Chaudhary, A., Dhanjal, J.K., Dewanjee, S., Vallamkondu, J., Pérez de la Lastra, J.M., 2023. Cancer chemotherapy and beyond: current status, drug candidates, associated risks and progress in targeted therapeutics. Genes. Dis. 10, 1367–1401. https://doi.org/10.1016/J.GENDIS.2022.02.007.

Asaduzzaman, M., Uddin, M.J., Kader, M.A., Alam, A.H.M.K., Rahman, A.A., Rashid, M., Kato, K., Tanaka, T., Takeda, M., Sadik, G., 2014. In vitro acetylcholinesterase inhibitory activity and the antioxidant properties of Aegle marmelos leaf extract: implications for the treatment of Alzheimer's disease. Psychogeriatrics. 14, 1–10. https://doi.org/10.1111/PSYG.12031.

Asma, S.T., Acaroz, U., Imre, K., Morar, A., Shah, S.R.A., Hussain, S.Z., Arslan-Acaroz, D., Demirbas, H., Hajrulai-Musliu, Z., Istanbullugil, F.R., Soleimanzadeh, A., Morozov, D., Zhu, K., Herman, V., Ayad, A., Athanassiou, C., Ince, S., 2022. Natural products/bioactive compounds as a source of anticancer drugs. Cancers 2022 14, 6203. https://doi.org/10.3390/CANCERS14246203. Page14, 6203.

Ayertey, F., Ofori-Attah, E., Antwi, S., Amoa-Bosompem, M., Djameh, G., Lartey, N.L., Ohashi, M., Kusi, K.A., Appiah, A.A., Appiah-Opong, R., Okine, L.K., 2021. Anti-inflammatory activity and mechanism of action of ethanolic leaf extract of Morinda lucida Benth. J. Tradit. Complement. Med. 11, 249–258. https://doi.org/10.1016/J.JTCME.2020.07.001.

Bhattarai, N., Kumbhar, A.A., Pokharel, Y.R., Yadav, P.N., 2021. Anticancer potential of Coumarin and its derivatives. Mini-Rev. Med. Chem. 21, 2996–3029. https://doi.org/10.2174/1389557521666210405160323/CITE/REFWORKS.

Borquaye, L.S., Laryea, M.K., Gasu, E.N., Boateng, M.A., Baffour, P.K., Kyerematen, A., Doh, G., 2020. Anti-inflammatory and antioxidant activities of extracts of Reissantia indica, Cissus cornifolia and Grosseria vignei. Cogent. Biol. 6, 1785755. https://doi.org/10.1080/23312025.2020.1785755.

Chauhan, A., Dubey, S., Jain, S., 2024. Association between type 2 Diabetes Mellitus and Alzheimer's Disease: common molecular mechanism and therapeutic targets. Cell Biochem. Funct. 42, e4111. https://doi.org/10.1002/CBF.4111.

Chimento, A., De Luca, A., D'Amico, M., De Amicis, F., Pezzi, V., 2023. The involvement of natural polyphenols in molecular mechanisms inducing apoptosis in tumor cells: a promising adjuvant in cancer therapy. Int. J. Mol. Sci. 24, 1680. https://doi.org/10.3390/IJMS24021680.

Custodio, L., Garcia-Caparros, P., Pereira, C.G., Castelo-Branco, P., 2022. Halophyte plants as potential sources of anticancer agents: a comprehensive review. Pharmaceutics. 14, 2406. https://doi.org/10.3390/PHARMACEUTICS14112406.

Ellman, G.L., Courtney, K.D., Andres, V., Featherstone, R.M., 1961. A new and rapid colorimetric determination of acetylcholinesterase activity. Biochem. Pharmacol. 7, 88–95. https://doi.org/10.1016/0006-2952(61)90145-9.

El-Raouf, H.S.A., 2021. Taxonomic significance of leaves in family Aizoaceae. Saudi. J. Biol. Sci. 28, 512–522. https://doi.org/10.1016/J.SJBS.2020.10.036.

El-Saadony, M.T., Zabermawi, Nidal M., Zabermawi, Nehal M., Burollus, M.A., Shafi, M. E., Alagawany, M., Yehia, N., Askar, A.M., Alsafy, S.A., Noreldin, A.E., Khafaga, A.F., Dhama, K., Elnesr, S.S., Elwan, H.A.M., Cerbo, A.Di, El-Tarabily, K.A., Abd El-Hack, M.E., 2023. Nutritional aspects and health benefits of bioactive plant compounds against infectious diseases: a review. Food Rev. Int. 39, 2138–2160. https://doi.org/10.1080/87559129.2021.1944183.

Flosadóttir, H.D., Jónsson, H., Sigurdsson, S.T., Ingólfsson, O., 2011. Experimental and theoretical study of the metastable decay of negatively charged nucleosides in the gas phase. Phys. Chem. Chem. Phys. 13, 15283–15290. https://doi.org/10.1039/C1CP21298B.

Gonfa, Y.H., Tessema, F.B., Bachheti, A., Rai, N., Tadesse, M.G., Nasser Singab, A., Chaubey, K.K., Bachheti, R.K., 2023. Anti-inflammatory activity of phytochemicals from medicinal plants and their nanoparticles: a review. Curr. Res. Biotechnol. 6, 100152. https://doi.org/10.1016/J.CRBIOT.2023.100152.

Guchhait, K.C., Manna, T., Barai, M., Karmakar, M., Nandi, S.K., Jana, D., Dey, A., Panda, S., Raul, P., Patra, A., Bhattacharya, R., Chatterjee, S., Panda, A.K., Ghosh, C., 2022. Antibiofilm and anticancer activities of unripe and ripe Azadirachta indica (neem) seed extracts. BMC. Complement. Med. Ther. 22, 1–18. https://doi.org/10.1186/S12906-022-03513-4/FIGURES/9.

Ha, S.K., Lee, J.A., Cho, E.J., Choi, I., 2017. Effects of catechol O-methyl transferase inhibition on anti-inflammatory activity of luteolin metabolites. J. Food Sci. 82, 545–552. https://doi.org/10.1111/1750-3841.13620.

Harnly, J.M., Bhagwat, S., Lin, L.Z., 2007. Profiling methods for the determination of phenolic compounds in foods and dietary supplements. Anal. Bioanal. Chem. 389, 47–61. https://doi.org/10.1007/S00216-007-1424-7/FIGURES/5.

Harper, P., 2023. A review of the dietary intake, bioavailability and health benefits of ellagic acid (EA) with a primary focus on its anti-cancer properties. Cureus. https://doi.org/10.7759/CUREUS.43156.

Hokkanen, J., Mattila, S., Jaakola, L., Pirttilä, A.M., Tolonen, A., 2009. Identification of phenolic compounds from lingonberry (Vaccinium vitis-idaea L.), bilberry (Vaccinium myrtillus L.) andHybrid bilberry (Vaccinium x intermedium Ruthe L.) leaves. J. Agric. Food Chem. 57, 9437–9447. https://doi.org/10.1021/JF9022542/ASSET/IMAGES/LARGE/JF-2009-022542_0001.JPEG.

Huang, Q., Liao, C., Ge, F., Ao, J., Liu, T., 2022. Acetylcholine bidirectionally regulates learning and memory. J. Neurorestoratol. 10, 100002. https://doi.org/10.1016/J.JNRT.2022.100002.

Ibrahim, R.M., Eltanany, M., B, Pont, L., Benavente, F., ElBanna, S.A., Otify, A.M., 2023. Unveiling the functional components and antivirulence activity of mustard leaves using an LC-MS/MS, molecular networking, and multivariate data analysis integrated approach. Food Res. Int. 168, 112742. https://doi.org/10.1016/J.FOODRES.2023.112742.

Jiang, H., Sólyom, A.M., Timmermann, B.N., Gang, D.R., 2005. Characterization of gingerol-related compounds in ginger rhizome (Zingiber officinale Rosc.) by high-performance liquid chromatography/electrospray ionization mass spectrometry. Rapid Commun. Mass Spectrom. 19, 2957–2964. https://doi.org/10.1002/RCM.2140.

Jimoh, M.O., Kerebba, N., Okechukwu, O.C., Jimoh, A.A., Salaudeen, T., Bamigboye, S. O., Sogoni, A., Okaiyeto, K., Mkhwanazi, N., Kadye, R., Idris, O.A., Erasmus, M., Prinsloo, E., Laubscher, C.P., 2024. Analysis of antioxidant nutrients, anti-HIV and anticancer metabolic fingerprints of pelargonium quercifolium (L.f) L'Hér. Food Chem. Adv. 5, 100804. https://doi.org/10.1016/J.FOCHA.2024.100804.

Jo, H.M., Choi, I.H., 2024. Anti-inflammatory activity of Akebia quinata D. extracts by inhibiting MAPK and NF-κb signaling pathways in LPS-induced RAW 264.7 cells according to extraction solvents. Mol. Cell Toxicol. 21, 315–323. https://doi.org/10.1007/S13273-024-00477-Z/FIGURES/5.

Jolad, S.D., Lantz, R.C., Solyom, A.M., Chen, G.J., Bates, R.B., Timmermann, B.N., 2004. Fresh organically grown ginger (Zingiber officinale): composition and effects on LPS-induced PGE2 production. Phytochemistry 65, 1937–1954. https://doi.org/10.1016/J.PHYTOCHEM.2004.06.008.

Kerebba, N., Oyedeji, A.O., Byamukama, R., Kuria, S.K., Oyedeji, O.O., 2022. UHPLC-ESI-QTOF-MS/MS characterisation of phenolic compounds from Tithonia diversifolia (Hemsl.) A. Gray and antioxidant activity. ChemistrySelect. 7, e202104406. https://doi.org/10.1002/SLCT.202104406.

Khalili, M., Alavi, M., Esmaeil-Jamaat, E., Baluchnejadmojarad, T., Roghani, M., 2018. Trigonelline mitigates lipopolysaccharide-induced learning and memory impairment in the rat due to its anti-oxidative and anti-inflammatory effect. Int. Immunopharmacol. 61, 355–362. https://doi.org/10.1016/J.INTIMP.2018.06.019.

Kim, H.R., Noh, E.M., Lee, S.H., Lee, S., Kim, D.H., Lee, N.H., Kim, S.Y., Park, M.H., 2024. Momordica charantia extracts obtained by ultrasound-assisted extraction inhibit the inflammatory pathways. Mol. Cell Toxicol. 20, 67–74. https://doi.org/10.1007/S13273-022-00320-3/FIGURES/6.

Kramberger, K., Barlič-Maganja, D., Bandelj, D., Baruca Arbeiter, A., Peeters, K., Miklavčič Višnjevec, A., Pražnikar, Z.J., 2020. HPLC-DAD-ESI-QTOF-MS determination of bioactive compounds and antioxidant activity comparison of the hydroalcoholic and water extracts from two helichrysum italicum species. Metab. 2020 10, 403. https://doi.org/10.3390/METABO10100403. Page10, 403.

Liang, Y., Xie, S., He, Y., Xu, M., Qiao, X., Zhu, Y., Wu, W., 2022. Kynurenine pathway metabolites as biomarkers in Alzheimer's disease. Dis. Markers 2022, 9484217. https://doi.org/10.1155/2022/9484217.

Maheshwari, N., Sharma, M.C., 2023. Anticancer properties of some selected plant phenolic compounds: future leads for therapeutic development. J. Herb. Med. 42, 100801. https://doi.org/10.1016/J.HERMED.2023.100801.

Mirzaei, S.A., Gholamian Dehkordi, N., Ghamghami, M., Amiri, A.H., Dalir Abdolahinia, E., Elahian, F., 2017. ABC-transporter blockage mediated by xanthotoxin and bergapten is the major pathway for chemosensitization of multidrug-resistant cancer cells. Toxicol. Appl. Pharmacol. 337, 22–29. https://doi.org/10.1016/J.TAAP.2017.10.018.

Mohammed, H.A., Emwas, A.H., Khan, R.A., 2023. Salt-tolerant plants, halophytes, as renewable natural resources for cancer prevention and treatment: roles of phenolics and flavonoids in immunomodulation and suppression of oxidative stress towards cancer management. Int. J. Mol. Sci. 24, 5171. https://doi.org/10.3390/IJMS24065171.

Nethengwe, M., Kerebba, N., Okaiyeto, K., Opuwari, C.S., Oguntibeju, O.O., 2024. Antioxidant, anti-diabetic, and anti-inflammation activity of Garcinia livingstonei aqueous leaf Extract: a preliminary study. Int. J. Mol. Sci. 2024 25, 3184. https://doi.org/10.3390/IJMS25063184.

Nguyen, T.T., Ta, Q.T.H., Nguyen, T.K.O., Nguyen, T.T.D., Giau, V.Van, 2020. Type 3 diabetes and its role implications in Alzheimer's disease. Int. J. Mol. Sci. 21, 3165. https://doi.org/10.3390/IJMS21093165.

Ngxabi, S., Jimoh, M.O., Sogoni, A., Laubscher, C.P., Rautenbach, F., Kambizi, L., 2025. Salinity influenced proximate, minerals, anti-nutrients and phytochemical composition of Trachyandra ciliata Kunth (Wild Cabbage): a promising edible halophyte. Food Sci. Nutr. 13, e4755. https://doi.org/10.1002/FSN3.4755.

Nkemzi, Achasih Quinta, Okaiyeto, K., Kerebba, N., Rautenbach, F., Oyenihi, O., Ekpo, O.E., Oguntibeju, O.O., 2024. In vitro hypoglycemic, antioxidant, anti-inflammatory activities and phytochemical profiling of aqueous and ethanol extracts of helichrysum cymosum. Phytomed. Plus. 4, 100639. https://doi.org/10.1016/J.PHYPLU.2024.100639.

Oguntibeju, O.O., 2018. Medicinal plants with anti-inflammatory activities from selected countries and regions of africa. J. Inflamm. Res. 11, 307–317. https://doi.org/10.2147/JIR.S167789.

Okaiyeto, K., Kerebba, N., Rautenbach, F., Kumar Singh, S., Dua, K., Oguntibeju, O.O., 2023. UPLC-ESI-QTOF-MS phenolic compounds identification and quantification from ethanolic extract of Myrtus communis 'Variegatha': in vitro antioxidant and antidiabetic potentials. Arab. J. Chem. 16, 104447. https://doi.org/10.1016/J.ARABJC.2022.104447.

Park, S.Y., Jung, M.Y., 2016. UHPLC-ESI-MS/MS for the Quantification of Eight Major Gingerols and Shogaols in Ginger Products: Effects of Ionization Polarity and Mobile Phase Modifier on the Sensitivity. J. Food Sci. 81, C2457– C2465. https://doi.org/10.1111/1750-3841.13429.

Pintatum, A., Maneerat, W., Logie, E., Tuenter, E., Sakavitsi, M.E., Pieters, L., Berghe, W. Vanden, Sripisut, T., Deachathai, S., Laphookhieo, S., 2020. Vitro anti-inflammatory, anti-oxidant, and cytotoxic activities of four Curcuma species and the isolation of compounds from curcuma aromatica rhizome. Biomol. 2020 10, 799. https://doi.org/10.3390/BIOM10050799. Page10, 799.

Piotrowska, H., Kucinska, M., Murias, M., 2012. Biological activity of piceatannol: leaving the shadow of resveratrol. Mutat. Res./Rev. Mutat. Res. 750, 60–82. https://doi.org/10.1016/J.MRREV.2011.11.001.

Powell, R.F., Magee, A.R., Boatwright, J.S., 2018. Decoding ice plants: challenges associated with barcoding and phylogenetics in the diverse succulent family Aizoaceae. Genome 61, 815–821. https://doi.org/10.1139/GEN-2018-0055.

Prasathkumar, M., Becky, R., Anisha, S., Dhrisya, C., Sadhasivam, S., 2022. Evaluation of hypoglycemic therapeutics and nutritional supplementation for type 2 diabetes mellitus management: an insight on molecular approaches. Biotechnol. Lett. 2022 44 (2), 44. https://doi.org/10.1007/S10529-022-03232-3, 203–238.

Prinsloo, S., Pieters, R., Bezuidenhout, C.C., 2013. A cell viability assay to determine the cytotoxic effects of water contaminated by microbes. S. Afr. J. Sci. 109. https://doi.org/10.1590/SAJS.2013/20120069.

Promdam, N., Panichayupakaranant, P., 2022. [6]-Gingerol: a narrative review of its beneficial effect on human health. Food Chem. Adv. 1, 100043. https://doi.org/10.1016/J.FOCHA.2022.100043.

Rani, A., Khan, J., Choudhary, L., Kumar, M., Jha, A., Pandey, G., Nand, B., 2025. Unraveling the synthesis and therapeutic potential of FDA-approved Alzheimer's drugs: a comprehensive review. Tetrahedron. 175, 134517. https://doi.org/10.1016/J.TET.2025.134517.

Salari, Z., Khosravi, A., Pourkhandani, E., Molaakbari, E., Salarkia, E., Keyhani, A., Sharifi, I., Tavakkoli, H., Sohbati, S., Dabiri, S., Ren, G., Shafie'ei, M., 2023. The inhibitory effect of 6-gingerol and cisplatin on ovarian cancer and antitumor activity: in silico, in vitro, and in vivo. Front. Oncol. 13, 1098429. https://doi.org/10.3389/FONC.2023.1098429/BIBTEX.

Sharma, V.K., Singh, T.G., Prabhakar, N.K., Mannan, A., 2022. Kynurenine metabolism and Alzheimer's disease: the potential targets and approaches. Neurochem. Res. 2022 47 (6), 47. https://doi.org/10.1007/S11064-022-03546-8, 1459–1476.

Shoaib, M., Shah, I., Ali, N., Adhikari, A., Tahir, M.N., Shah, S.W.A., Ishtiaq, S., Khan, J., Khan, S., Umer, M.N., 2017. Sesquiterpene lactone! a promising antioxidant, anticancer and moderate antinociceptive agent from Artemisia macrocephala jacquem. BMC. Complement. Altern. Med. 17, 1–11. https://doi.org/10.1186/S12906-016-1517-Y/TABLES/6.

Silva, D., Ferreira, M.S., Sousa-Lobo, J.M., Cruz, M.T., Almeida, I.F., 2021. Anti-inflammatory activity of Calendula officinalis L. Flower extract. Cosmet. 2021 8, 31. https://doi.org/10.3390/COSMETICS8020031. Page8, 31.

Soerjomataram, I., Cabasag, C., Bardot, A., Fidler-Benaoudia, M.M., Miranda-Filho, A., Ferlay, J., Parkin, D.M., Ranganathan, R., Piñeros, M., Znaor, A., Mery, L., Joko-Fru, Y.W., Dikshit, R., Sankaranarayanan, R., Swaminathan, R., Bray, F., 2023. Cancer survival in Africa, central and south America, and Asia (SURVCAN-3): a population-based benchmarking study in 32 countries. Lancet Oncol. 24, 22–32. https://doi.org/10.1016/S1470-2045(22)00704-5.

Sogoni, A., Jimoh, M.O., Laubscher, C.P., Kambizi, L., 2022. Effect of rooting media and IBA treatment on rooting response of South African dune spinach (Tetragonia decumbens): an underutilized edible halophyte. Acta Horticulturae. International Society for Horticultural Science, pp. 319–325. https://doi.org/10.17660/ActaHortic.2022.1356.38.

Sogoni, A., Jimoh, M.O., Mngqawa, P., Ngxabi, S., Le Roes-Hill, M., Kambizi, L., Laubscher, C.P., 2024. Comparing the nutritional, phytochemical, and anti-microbial potential of wild and cultivated Tetragonia decumbens mill.: a promising leafy vegetable for bio-saline agriculture in South Africa. J. Agric. Food Res. 18, 101419. https://doi.org/10.1016/J.JAFR.2024.101419.

Sogoni, A., Jimoh, M.O., Ngxabi, S., Kambizi, L., Laubscher, C.P., 2025. Evaluating the nutritional, therapeutic, and economic potential of Tetragonia decumbens Mill.: a promising wild leafy vegetable for bio-saline agriculture in South Africa. Open. Agric. 10. https://doi.org/10.1515/OPAG-2022-0368.

Taqui, R., Debnath, M., Ahmed, S., Ghosh, A., 2022. Advances on plant extracts and phytocompounds with acetylcholinesterase inhibition activity for possible treatment of Alzheimer's disease. Phytomed. Plus 2, 100184. https://doi.org/10.1016/J.PHYPLU.2021.100184.

Uddin, M.J., Russo, D., Rahman, M.M., Uddin, S.B., Halim, M.A., Zidorn, C., Milella, L., 2021. Anticholinesterase activity of eight medicinal plant species: in Vitro and In Silico studies in the search for therapeutic agents against Alzheimer's disease. Evid.-Based Complement. Altern. Med. 2021, 9995614. https://doi.org/10.1155/2021/9995614.